Supplementary Information for: Comparison of gels synthesized by controlled radical copolymerization and free radical copolymerization: molecular dynamics simulation

Tsutomu Furuya* and Tsuyoshi Koga*

S1 Details of Simulation Method

S1.1 Reaction Process

Fig. S1 shows the flow chart of the actual calculation in the CRP in this simulation. We first select one bead (B_1) at random from the simulation box, and judge the type of B_1. We then perform the following calculations according to the type of B_1. If B_1 is an unreacted monomer or an unreacted end of a cross-linker, we randomly select another bead (B_2) within the distance r_c from B_1, and proceed to the next step if B_2 is a propagating end. If the propagating end B_2 becomes a radical with the probability P_a, the propagation process is executed with the probability p_p. If B_1 is a propagating end, B_1 is stochastically determined to be a radical (probability P_a) or a dormant species (probability $1-P_a$). If B_1 is a radical, we randomly select another bead (B_2) within the distance r_c from B_1, and perform the following calculations according to the type of B_2. If B_2 is an unreacted monomer or an unreacted end of a cross-linker, the propagation process is executed with the probability p_p. If B_2 is a propagating end, B_2 is stochastically determined to be a radical (P_a) or a dormant species ($1-P_a$), and the termination process is executed with the probability p_t if B_2 is a radical. The probabilities of the combination and the disproportionation when the termination process is executed are $p_t^{(c)}$ and $p_t^{(d)}$, respectively. We performed the trial shown in Fig. S1 n times at each simulation step. Here, n is the total number of beads in the simulation box.

S1.2 Details of Simulation Conditions

Table S1 lists the initial conditions for forming each gel and the number average molecular weights $M_{n,p}$ of the primary chains constituting each gel with the monomer conversion α of 95%.

S1.3 Calculation of Number Density ν_{te} of Elastically Effective Chains Generated by Trapped Entanglements

The calculation of the number density ν_{te} of elastically effective chains generated by entanglements trapped in the network was performed in the same way as in the previous studies.[1,2] By the method of Everaers *et al.*[3], we first extracted the primitive paths that connect the ends of each polymer without crossing between the polymers, and then counted the number of the contact points of the primitive paths as entanglements. We spatially fixed the ends of the polymers, turned off the intra-strand WCA potentials and the WCA potentials between the strands attached to the same crosslinking point, and then performed the simulation of $t = 1\times10^4\tau$ with decreasing the temperature T at a cooling rate $dT/dt = -1\times10^{-4}\varepsilon_{wca}/k_B\tau$. We then counted the number n_{en}

Department of Polymer Chemistry, Graduate School of Engineering, Kyoto University, Katsura, Kyoto 615-8510, Japan. E-mail: furuya.tsutomu.4a@kyoto-u.ac.jp, koga.tsuyoshi.6m@kyoto-u.ac.jp

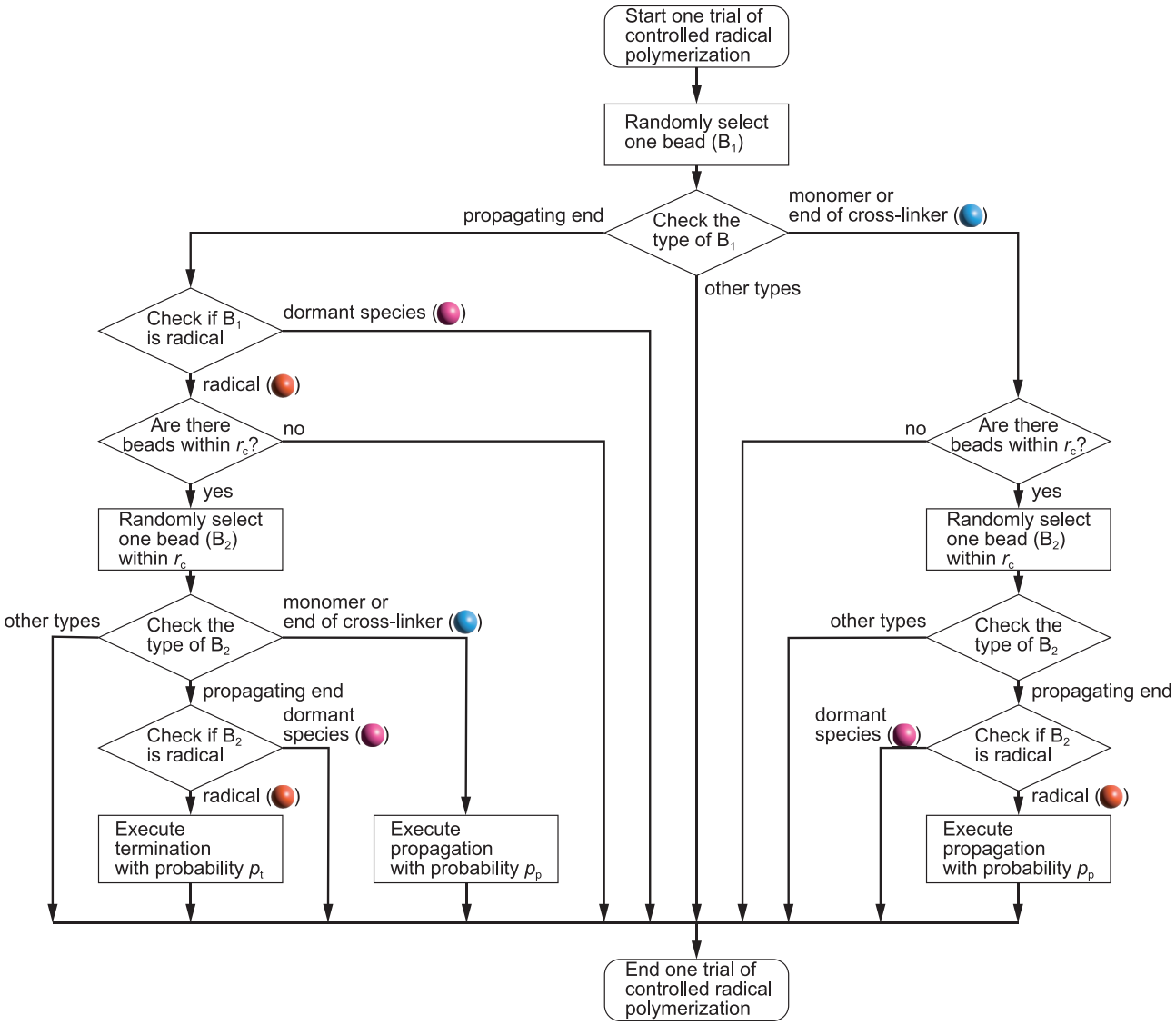

Figure S1 Flow chart of one trial of the controlled radical copolymerization process.

of entanglements and the number g_i $(i = 1, 2, \cdots, n_{en})$ of strands included in each entanglement. Here, an area where more than two strands simultaneously contact with each other was regarded as one entanglement. The number N_{en} of the bridge chains generated by the entanglements was calculated by $N_{en} = \sum_{i=1}^{n_{en}} g_i$.

The entanglements trapped in the network were analyzed with reference to Langley's criterion[4]. In Langley's criterion, the entanglements which contain two strands having paths to the network matrix at both sides of the entanglements are considered to be trapped in the networks and elastically effective. Therefore, the trapped entanglements have to contain two or more elastically effective chains. This is because the strands that are part of elastically ineffective chains are not connected to the network matrix at one or both ends of the path along the strands. In other words, the strands satisfying Langley's criterion must be at least part of the elastically effective chains. Using this criterion, we extracted the trapped entanglements from n_{en} entanglements and count the number $g_i'(i = 1, 2, \cdots, n_{te})$ of elastically effective strands included in each trapped entanglement. Here, n_{te} is the number of trapped entanglements. The number density ν_{te} of elastically effective chains generated by the trapped entanglements was calculated by $\nu_{te} = \sum_{i=1}^{n_{te}} g_i'/V$.

Table S1 Detailed initial conditions for gel formation and the number average molecular weight $M_{\mathrm{n,p}}$ of the primary chains at $\alpha = 95\%$.

system type	V	n_{m}	n_{x}	$n_{\mathrm{p-x}}$	n_{i}	$M_{\mathrm{n,p}}$ at $\alpha = 95\%$
FRP	$\simeq 5.24 \times 10^5$	1×10^5	2650	0	100	$\simeq 2.02 \times 10^3$
	$\simeq 5.24 \times 10^5$	1×10^5	2650	0	350	$\simeq 1.03 \times 10^3$
	$\simeq 5.24 \times 10^5$	1×10^5	2650	0	1400	$\simeq 0.51 \times 10^3$
LRP ($P_{\mathrm{a}} = 0.1$)	$\simeq 5.24 \times 10^5$	1×10^5	2650	50	0	$\simeq 2.03 \times 10^3$
	$\simeq 5.24 \times 10^5$	1×10^5	2650	100	0	$\simeq 1.01 \times 10^3$
	$\simeq 5.24 \times 10^5$	1×10^5	2650	200	0	$\simeq 0.51 \times 10^3$
LRP ($P_{\mathrm{a}} = 0.02$)	$\simeq 5.24 \times 10^5$	1×10^5	2650	50	0	$\simeq 2.00 \times 10^3$
	$\simeq 5.24 \times 10^5$	1×10^5	2650	100	0	$\simeq 1.00 \times 10^3$
	$\simeq 5.24 \times 10^5$	1×10^5	2650	200	0	$\simeq 0.50 \times 10^3$
LRP ($P_{\mathrm{a}} = 0.01$)	$\simeq 5.24 \times 10^5$	1×10^5	2650	50	0	$\simeq 2.00 \times 10^3$
	$\simeq 5.24 \times 10^5$	1×10^5	2650	100	0	$\simeq 1.00 \times 10^3$
	$\simeq 5.24 \times 10^5$	1×10^5	2650	200	0	$\simeq 0.50 \times 10^3$
FRPfi	$\simeq 5.24 \times 10^5$	1×10^5	2650	0	25	$\simeq 2.12 \times 10^3$
	$\simeq 5.24 \times 10^5$	1×10^5	2650	0	50	$\simeq 1.07 \times 10^3$
	$\simeq 5.24 \times 10^5$	1×10^5	2650	0	100	$\simeq 0.54 \times 10^3$
FRPsp	$\simeq 5.24 \times 10^5$	1×10^5	2650	0	75	$\simeq 1.02 \times 10^3$
	$\simeq 5.24 \times 10^5$	1×10^5	2650	0	230	$\simeq 0.46 \times 10^3$
FRPwot	$\simeq 5.24 \times 10^5$	1×10^5	2650	0	130	$\simeq 2.01 \times 10^3$
	$\simeq 5.24 \times 10^5$	1×10^5	2650	0	550	$\simeq 0.99 \times 10^3$
	$\simeq 5.24 \times 10^5$	1×10^5	2650	0	2290	$\simeq 0.51 \times 10^3$
FRPfiwot	$\simeq 5.24 \times 10^5$	1×10^5	2650	0	25	$\simeq 2.00 \times 10^3$
	$\simeq 5.24 \times 10^5$	1×10^5	2650	0	50	$\simeq 1.00 \times 10^3$
	$\simeq 5.24 \times 10^5$	1×10^5	2650	0	100	$\simeq 0.50 \times 10^3$

V: volume of simulation box; n_{m}: initial number of monomers; n_{x}: initial number of cross-linkers; $n_{\mathrm{p-x}}$: initial number of dormant species; n_{i}: initial number of initiators; $M_{\mathrm{n,p}}$: number average molecular weight of primary chains.

S1.4 Calculation of Static Structure Factor $S(q)$

In order to calculate the structure factor $S(q)$ in the network formation process, we first carried out the simulation with the polymerization until α reached a target value, and then performed the simulation of $t = 5.5 \times 10^3 \tau$ without processing the reaction. In the last $5 \times 10^3 \tau$ of this simulation, the structure factor was calculated by the following equation every 50τ:

$$S(\boldsymbol{q}) = \left| \sum_{j=1}^{n} \exp\left(i\boldsymbol{q} \cdot \boldsymbol{r}_j\right) \right|^2, \tag{S1}$$

$$S(q) = \frac{1}{4\pi q^2} \int S(\boldsymbol{q}) \delta(|\boldsymbol{q}| - q) d\boldsymbol{q}, \tag{S2}$$

where, $\boldsymbol{q} = (2\pi/L_0)(k,l,m)$ (k, l, and m are integer) is the scattering vector, and $\boldsymbol{r}_j$ is the position vector of the j-th bead. The average of the 100 calculation results was taken as the result of one run, and the average of the results of ten independent runs was taken as the result for each condition.

S2 Supplementary Information about Simulation

S2.1 Polymerization of Linear Polymers

In order to check the behavior of the FRP model and the CRP model, we here present the results of the polymerization of linear polymers in the systems without the cross-linkers ($n_\mathrm{x} = 0$). Figs. S2a–S2c show the time developments of the concentrations of each species, and Figs. S2d–S2f depict the time developments of the monomer conversion α and the conversion index (CI) $\ln[\mathrm{M}]_0/\mathrm{M}$. In Figs. S2g–S2i, we plot the number average molecular weight M_n, the weight average molecular weight M_w, and the polydispersity index (PDI) $M_\mathrm{w}/M_\mathrm{n}$ against α. Here, the initial monomer concentration $[\mathrm{M}]_0$ is set to $[\mathrm{M}]_0 \simeq 0.19$ ($\phi_\mathrm{m} = 0.1$), the initial initiator concentration $[\mathrm{I}]_0$ for the FRP is set to $[\mathrm{I}]_0 \simeq 6.7 \times 10^{-4}$ ($n_\mathrm{i} = 350$), and the initial dormant species concentration $[\mathrm{P\text{–}X}]_0$ for the CRPs is set to $[\mathrm{P\text{–}X}]_0 \simeq 1.9 \times 10^{-4}$ ($n_{\mathrm{p-x}} = 100$).

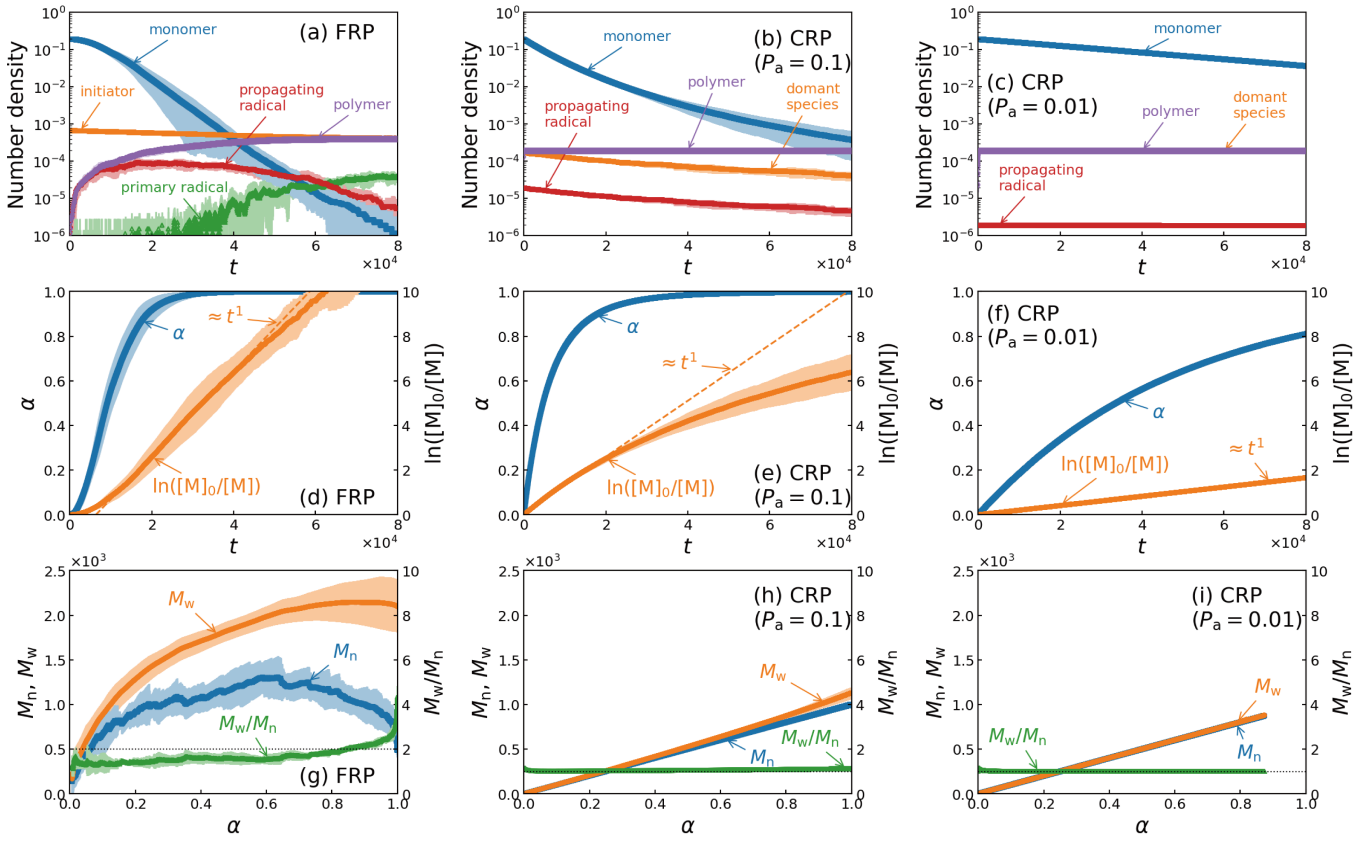

Figure S2 Time developments of (a–c) the number densities of each species, (d–f) the monomer conversion α, and the conversion index $\ln[\mathrm{M}]_0/[\mathrm{M}]$. (g–i) Number average molecular weight M_n, weight average molecular weight M_w, and polydispersity index $M_\mathrm{w}/M_\mathrm{n}$ shown as functions of α.

As discussed in detail in the previous study[2], we think that the results of the FRP reproduce some features of the kinetics of FRP.[5] The concentration of propagating radicals is almost constant in the time region of $1 \times 10^4 \lesssim t \lesssim 4 \times 10^4$ (Fig. S2a); thus, this time range is considered to correspond the steady state. In the steady state the CI is approximately proportional to t (Fig. S2d). We have also confirmed that the propagation rate $R_\mathrm{p} = -d[\mathrm{M}]/dt$ in the initial stage is proportional to $[\mathrm{I}]_0^a[\mathrm{M}]_0^b$ and the reaction orders are $a \simeq 0.6$ and $b \simeq 0.9$–1.2, which are in agreement with the kinetics of FRP ($a = 1/2$ and $b = 1$). The average molecular weights M_n and M_w indicate large values from the early stage of the polymerization, and the PDI exhibits values close to two, which is the theoretical value, over a wide range (Fig. S2g). In addition, we have confirmed that both M_n and M_w are proportional to $[\mathrm{I}]_0^c[\mathrm{M}]_0^d$, and the exponents are $c \simeq -0.6$–-0.5 and $d \simeq 1.0$–1.3 for M_n

and $c \simeq -0.6$–-0.5 and $d \simeq 1.1$–1.4 for M_w. These exponents are also consistent with the kinetics of FRP when the termination mechanism is mainly the disproportionation: $c = -1/2$ and $d = 1$.

Let us discuss the reaction rate constants to compare the simulation with real FRPs. The reaction rate constants of each elementary reaction in the simulation evaluated using the time evolution of the concentrations of each species and the kinetics of FRP are $k'_d \simeq 6.7 \times 10^{-6}$, $k_p \simeq 2.2$, and $k_t \simeq 3.3$.[2] Here, k'_d is the effective reaction rate constant of the initiator decomposition including the initiator efficiency, k_p and k_t are the reaction rate constants of the propagation and termination, respectively. In real FRPs, $k_t \gg k_p \gg k'_d$ (typical values are $k'_d \simeq 1 \times 10^{-5}$ s^{-1}, $k_p \simeq 1 \times 10^3$ L mol^{-1} s^{-1}, and $k_t \simeq 1 \times 10^7$ L mol^{-1} s^{-1}),[5] but in the simulation, $k_t > k_p \gg k'_d$. Therefore, the termination in the simulation is slower than that in real FRPs. Although $k_t \gg k_p$ in real FRPs, in order to avoid unrealistically long calculation times, we here set the reaction probabilities focusing on the slow initiation and very fast propagation relative to the initiation.

We think that the results of the CRPs also reproduce some features of the kinetics of CRP with the dissociation-combination mechanism having a large number of stable radicals or the atom transfer mechanism having a large number of deactivators.[5,6] In the CRP with $P_a = 0.01$, the CI is proportional to t; hence, the polymerization follows first-order kinetics (Fig. S2f). M_n and M_w are proportional to α, and the PDI is approximately one (Fig. S2i). In the CRP with $P_a = 0.1$, since the termination proceeds to some extent, the concentration of propagating ends decreases (Fig. S2b). As a result, the CI deviates from the ideal line proportional to t (Fig. S2e), and the PDI increases (Fig. S2h).

Fig. S3 shows the mean square displacement $\langle|\Delta \boldsymbol{r}(t)|^2\rangle$ of the unreacted monomers and propagating ends at various α. The diffusion of unreacted monomers is almost independent of α, but the diffusion of propagating ends is suppressed by increasing α. Due to the suppressed diffusion of the propagating ends, R_p of the FRP nonmonotonically changes with increasing α (Fig. S4). The increase in R_p around $\alpha \simeq 0.25$ is thought to be caused by the suppression of the termination, which is a bimolecular reaction of the propagating ends. At high α, R_p decreases because the propagation is also affected by the suppressed diffusion of the propagating ends. On the other hand, in the CRP, since the effect of the termination is small, R_p monotonically decreases with suppressing the diffusion of propagating ends. In the systems with the cross-linkers, although the diffusion of the propagating ends is further suppressed, $\langle|\Delta \boldsymbol{r}(t)|^2\rangle$ shows similar results to Fig. S3.

S2.2 Conversion of Functional Group of Cross-linker

Fig. S5 shows the conversion α_x of the functional group of the cross-linker and the ratio $n_{x,in}/n_x$ of the number of cross-linkers incorporated in the polymers to the total number of cross-linkers in the system as function of the monomer conversion α. Here, $n_{x,in}$ is the number of cross-linkers incorporated in the polymers. α_x is lower than α, but $n_{x,in}/n_x$ is higher than α. These results indicate that many functional groups of the cross-linkers remain unreacted in the polymers. Therefore, we think that the difference between α_x and α is caused by the decrease in reactivity of the pendant group due to steric hindrance.

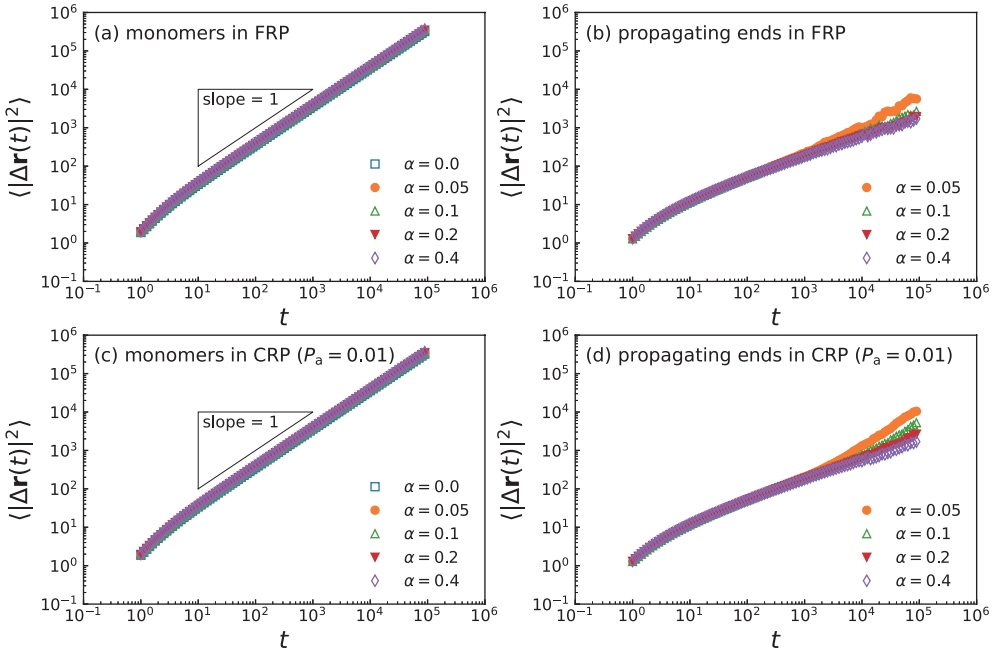

Figure S3 Mean square displacement $\langle|\Delta \boldsymbol{r}(t)|^2\rangle$ of (a, c) the unreacted monomers and (b, d) propagating ends.

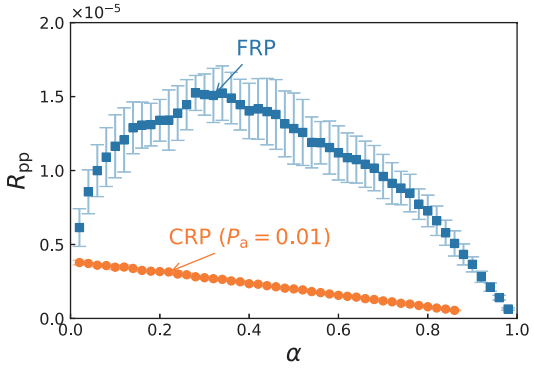

Figure S4 Propagation rate R_p shown as a function of the monomer conversion α.

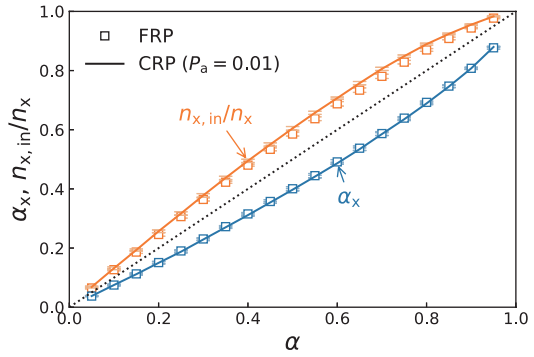

Figure S5 Conversion α_x of the functional group of the cross-linker and ratio $n_{x,in}/n_x$ of the number of cross-linkers incorporated in the polymers to the total number of cross-linkers in the system as functions of the monomer conversion α.

S2.3 Results for Gels with Different $M_{n,p}$

In Fig. S6, we show the results for gels with $M_{n,p} \simeq 5 \times 10^2$ and $M_{n,p} \simeq 2 \times 10^3$. Here, we set $[I]_0$ to $[I]_0 \simeq 2.7 \times 10^{-3}$ ($n_i = 1400$) and $[I]_0 \simeq 1.9 \times 10^{-4}$ ($n_i = 100$) to form the FRP gels with $M_{n,p} \simeq 5 \times 10^2$ and $M_{n,p} \simeq 2 \times 10^3$, respectively. $[P\text{–}X]_0$ for the formation of the CRP gels with $M_{n,p} \simeq 5 \times 10^2$ and $M_{n,p} \simeq 2 \times 10^3$ are set to $[P\text{–}X]_0 \simeq 3.8 \times 10^{-4}$ ($n_{p-x} = 200$) and $[P\text{–}X]_0 \simeq 9.5 \times 10^{-5}$ ($n_{p-x} = 50$), respectively. By changing the synthesis method from the FRP to the CRP and reducing P_a, ν_x increases, and ν_{te} decreases. The shear modulus G does not significantly change in the results of the gels with $M_{n,p} \simeq 2 \times 10^3$, but it shows a tendency to decrease with the change of the synthesis method from the FRP to the CRP in the results of the gels with $M_{n,p} \simeq 5 \times 10^2$.

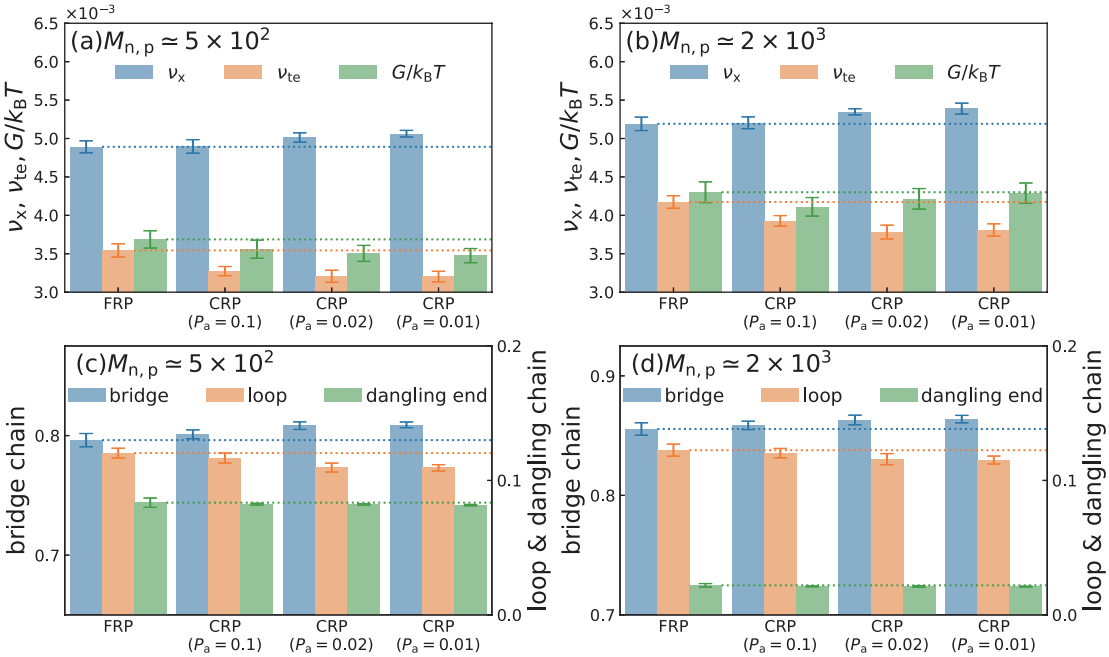

Figure S6 (a, b) Number density ν_x of the elastically effective chains formed by cross-linking, number density ν_{te} of the elastically effective chains generated by the trapped entanglements, and shear modulus G. (c, d) Relative populations of bridges, loops, and dangling ends. The number average molecular weight $M_{n,p}$ of the primary chains are set to (a, c) $M_{n,p} \simeq 5 \times 10^2$ and (b, d) $M_{n,p} \simeq 2 \times 10^3$. The monomer conversion is $\alpha = 95\%$. Dotted lines indicate the average values of the FRP gel.

In order to study the relationship between G and the network structure, we evaluate the contribution $G_x = (\nu_x - \mu_x)k_BT$ of the elastically effective cross-linking points and the contribution $G_{te} = (\nu_{te} - \mu_{te})k_BT$ of the trapped entanglements by using the phantom network model,[7,8] and plot G against $G_x + G_{te}$ (Fig. S7). Here, μ_x and μ_{te} are the number densities of the elastically effective cross-linking points and the trapped entanglements, respectively. From Fig. S7, we find that, although $G_x + G_{te}$ is about 20% larger than G, G is almost proportional to $G_x + G_{te}$. Therefore, within the simulation conditions, the behavior of G is considered to be explained by the elastically effective chains and the trapped entanglements. We think the difference between G and $G_x + G_{te}$ is caused by the effects of very short network strands. We think that such a very short strand does not serve as an independent elastically effective chain but as a part of a cross-linking point. Therefore, the presence of very short strands causes the overestimation of $G_x + G_{te}$.

S2.4 Results for Systems with Termination by Combination

Fig. S8 shows the results of the network structure and the number average molecular weight $M_{n,p}$ of the primary chains of gels with $\alpha = 95\%$ formed in systems in which the termination mechanism

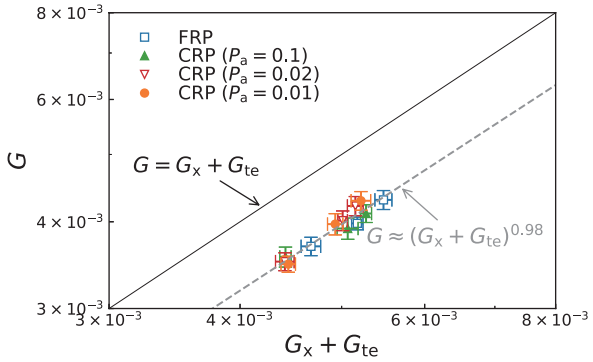

Figure S7 Shear modulus G calculated by the simulation under the uniaxial deformation shown as a function of the shear modulus $G_x + G_{te}$ evaluated from the network structure.

is the combination ($p_t^{(c)} = 1$ and $p_t^{(d)} = 0$). Here, $[\text{P–X}]_0$ and $[\text{I}]_0$ are set to the same values as those used in the calculation of Fig. 3 in the main text. Although $M_{n,p}$ of the FRP gel and the CRP gel with $P_a = 0.1$ are larger than 1.0×10^3 due to the effects of the termination, by changing the gel synthesis method from the FRP to the CRP and reducing P_a, the number density ν_x of the elastically effective chains formed by cross-linking increases, and the number density ν_{te} of the elastically effective chains generated by the trapped entanglements decreases. Thus, even if the termination is the combination, the homogeneity of the network structure is improved by changing the synthesis method from FRP to CRP.

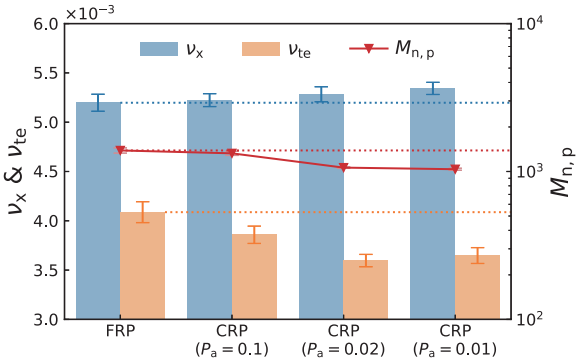

Figure S8 Number density ν_x of the elastically effective chains formed by cross-linking, number density ν_{te} of the elastically effective chains generated by the trapped entanglements, and number average molecular weight $M_{n,p}$ of the primary chains. The monomer conversion is $\alpha = 95\%$. Dotted lines indicate the average values of the FRP gel.

S2.5 Number of Entanglements in Gelation Process

Fig. S9 shows the number density $\tilde{\nu}_{en} \equiv N_{en}/V_{cls}$ of the bridge chains generated by the entanglements in clusters formed in the gelation process. Here, N_{en} is the number of bridge chains generated by the entanglements,[2] and V_{cls} is the total volume of the clusters, which is the total volume of beads constituting the clusters. Especially in the pre-gel region, the clusters in the FRP have more entanglements than the clusters in the CRP.

S2.6 Propagation Rate of FRPsp

Fig. S10a shows the propagation rates R_p of the CRP with $P_a = 0.01$ and FRPsp as functions of α. We can see that R_p of FRPsp is slower than that of the CRP ($P_a = 0.01$) throughout the polymerization.

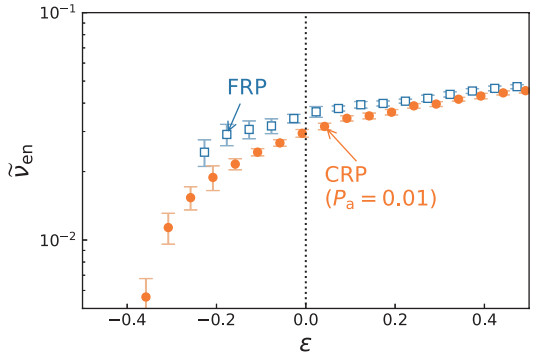

Figure S9 Number density $\tilde{\nu}_{en}$ of the bridge chains generated by the entanglements in the clusters. $M_{n,p} \simeq 1 \times 10^3$ at $\alpha = 95\%$.

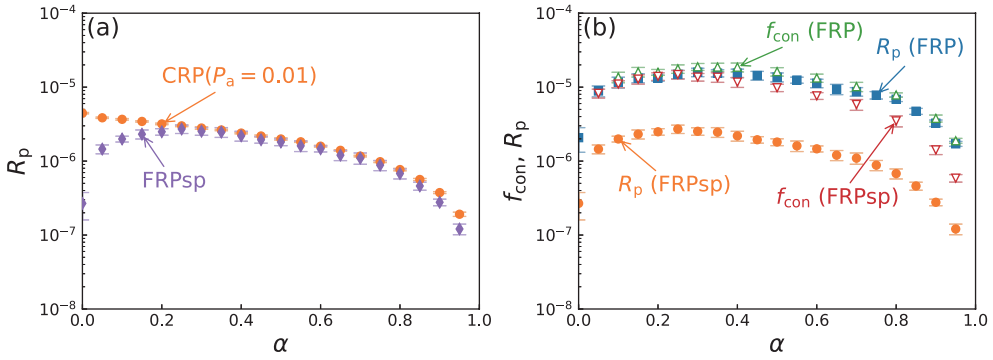

Figure S10 (a) Comparison of the propagation rate R_p between the CRP with $P_a = 0.01$ and FRPsp. (b) Contact frequencies f_{con} between the propagating radicals and the monomers, and propagation rates R_p for the FRP and FRPsp. $M_{n,p} \simeq 1 \times 10^3$ at $\alpha = 95\%$.

In order to study the relation between the propagation rate and the diffusion of the beads, we calculate the frequency of contact between the propagating radicals and the monomers. Specifically, we first carried out the simulation with the polymerization until α reached a target value, and then performed the simulation of $t = 5 \times 10^3 \tau$ without processing the reaction. The contact frequency $f_{con} = N_{con}/Vt_{ana}$ per unit volume was calculated from the contact number N_{con} between the propagating radicals and the monomers during the simulation without the reaction. Here, $t_{ana} = 5 \times 10^3 \tau$ is the time used for the calculation.

Fig. S10b shows f_{con} and R_p for the FRP and FRPsp as functions of α. In the FRP, since $R_p \simeq f_{con}$, the propagation is mainly determined by the contact between the propagating radicals and the monomers, *i.e.*, the propagation is diffusion-controlled. We here note that, since the time from contact to separation is $8\Delta t$–$10\Delta t$, $R_p \simeq f_{con}$ even if $p_p = 0.5$. On the other hand, in FRPsp with the slow propagation, since $R_p < f_{con}$, the propagation depends not only the contact between the beads but also on the stochastic reaction model.

S2.7 Structures of Network Strands and Clusters in Model Systems

In Fig. S11, we present the cross-linked structures of the network strands in the model systems. Fig. S12 shows the structures of clusters before and after gelation.

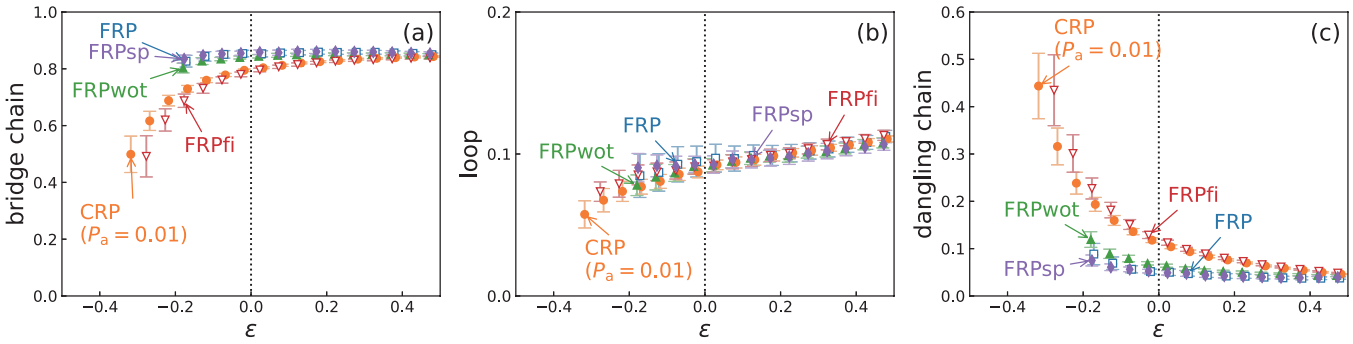

Figure S11 Relative populations of (a) bridges, (b) loops, and (c) dangling ends in clusters shown as functions of the distance ε from the gelation point. $M_{\mathrm{n,p}} \simeq 1 \times 10^3$ at $\alpha = 0.95$.

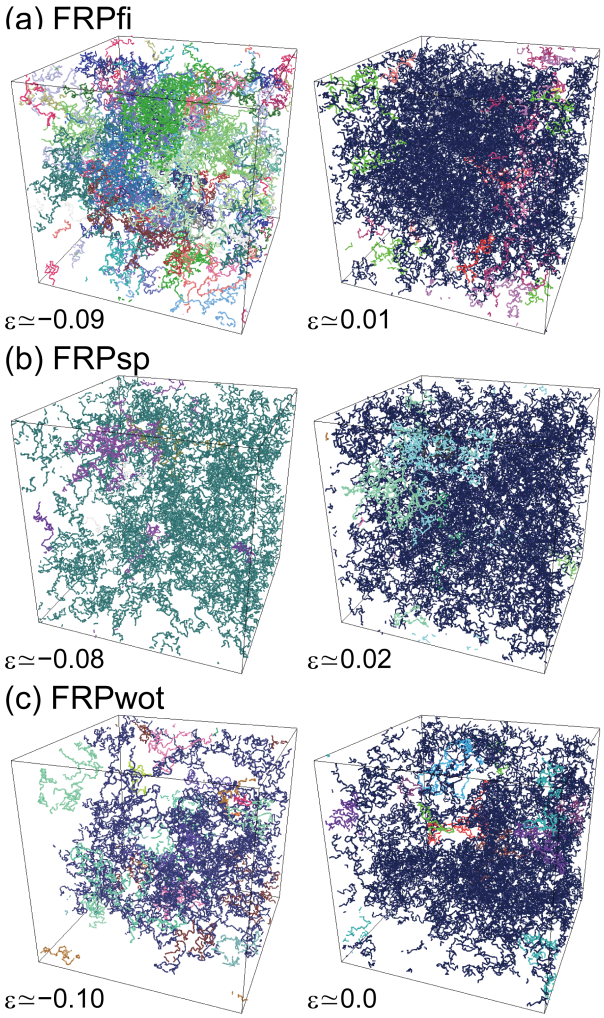

Figure S12 Structures of clusters at each distance ε from the gelation conversion in the (a) FRPfi, (b) FRPsp, and (b) FRPwot systems. Different clusters are shown in different colors.

S2.8 Results for a System with Fast Initiation and without Termination

We show the results of gels formed by a system with a fast initiation and without terminations ("FRPfiwot") on the ν_{x}-ν_{te} plane (Fig. S13). In FRPfiwot, the decomposition probability p_{d} of the initiator is set to one, and the termination probability p_{t} is set to zero. The results of the FRPfiwot

gel are shifted to the lower right direction compared to those of the FRPfi gel and FRPwot gel. Therefore, we find that the network structure is homogenized by prohibiting terminations in FRPfi with the fast initiation or by introducing the fast initiation in FRPwot without terminations. As shown in the main text, although the first initiation and the prohibition of terminations do not independently improve the homogeneity of the network structure, we think that these characteristics of CRP also contribute to the homogeneous structure of CRP gels.

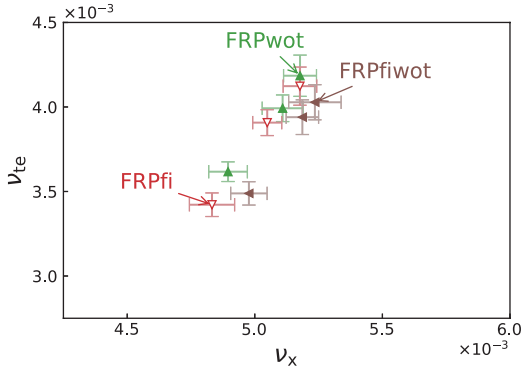

Figure S13 Number density ν_{te} of the elastically effective chains generated by the trapped entanglements plotted against the number density ν_x of the elastically effective chains formed by cross-linking. The monomer conversion is $\alpha = 95\%$.

References

[1] T. Furuya and T. Koga, *Macromol. Theory Simul.*, 2022, **31**, 2200044.

[2] T. Furuya and T. Koga, *Polymer*, 2023, **279**, 126012.

[3] R. Everaers, S. K. Sukumaran, G. S. Grest, C. Svaneborg, A. Sivasubramanian and K. Kremer, *Science*, 2004, **303**, 823–826.

[4] N. R. Langley, *Macromolecules*, 1968, **1**, 348–352.

[5] T. Endo, M. Sawamoto, M. Kamigaito, K. Satoh, S. Aoshima, S. Kanaoka, A. Hirao and K. Sugiyama, *Polymer synthesis*, Kodansha, Tokyo, Japan, 2010, vol. 1.

[6] A. Goto and T. Fukuda, *Prog. Polym. Sci.*, 2004, **29**, 329–385.

[7] H. M. James and E. Guth, *J. Chem. Phys.*, 1943, **11**, 455–481.

[8] P. J. Flory, *Proc. R. Soc. Lond. A*, 1976, **351**, 351–380.